Available online at www.sciencedirect.com
ScienceDirect
Journal of Power Sources 159 (2006) 1205–1213
JOURNAL OF POWER SOURCES
www.elsevier.com/locate/jpowsour

A fuel cell city bus with three drivetrain configurations

Junping Wang [a,c,*], Yong Chen [b,c], Quanshi Chen [c]

[a] *Key Laboratory of Education Ministry for Modern Design and Rotor-Bearing System, Xi'an Jiaotong University, Xi'an 710049, PR China*
[b] *School of Automobile and Transporting Engineering, Liaoning Institute of Technology, Jinzhou, Liaoning 121001, PR China*
[c] *State Key Laboratory of Automobile Safety & Energy Conservation, Tsinghua University, Beijing 100084, PR China*

Received 7 November 2005; received in revised form 6 December 2005; accepted 6 December 2005
Available online 17 February 2006

Abstract

Three fuel cell city buses of the energy hybrid- and power hybrid-type were re-engineered with three types of drivetrain configuration to optimize the structure and improve the performance. The energy distribution, hydrogen consumption, state of charge (SOC) and the power variation rate were analyzed when different drivetrain configurations and parameters were used. When powered only by a fuel cell, the bus cannot recover the energy through regenerative braking. The variation of the fuel cell power is large and frequent, which is not good for the fuel cell. When the fuel cell is linked to a battery pack in parallel, the bus can recover the energy through regenerative braking. The energy distribution is determined by the parameters of the fuel cell and the battery pack in the design stage to reduce the power variation rate of the fuel cell. When the fuel cell and DC/DC converter connected in series links the battery pack in parallel, energy can be recovered and the energy distribution can be adjusted online. The power variation rate of both the fuel cell and the battery pack are reduced.

Keywords: Fuel cell city bus; State of charge (SOC); Hydrogen consumption; Power variation rate

1. Introduction

The fuel cell powered city bus has attracted attention due to the benefit of low air pollution and high efficiency. Nearly every major automobile manufacturer in the world has stated an intention to introduce fuel cell powered city buses into the commercial marketplace during this decade [1]. Supported by the National High Technology Research and Development Program of China, Tsinghua University has developed three fuel cell buses during the past 3 years, collaborating with about 20 organizations of China from the year 2001–2004. These three fuel cell city buses were named the testbed bus, the practical bus A and the practical bus B. Fig. 1 shows the three buses. The design parameters are shown in Table 1.

At the beginning of the development, due to the limitations of the technology, the fuel cell power was too small to fulfill the entire vehicle power requirement. The fuel cell only provided power partially and the surplus power requirement was provided by other energy sources such as a battery pack. This kind of drivetrain configuration is the hybrid type and the testbed bus belongs to this. The lithium battery pack with a capacity of 100 Ah was used, which had a high specific energy and high specific power. The advantage of this drivetrain configuration is that the fuel cell can work in the range of nominal power with high efficiency, but a larger capacity battery pack is necessary as the weigh increases and the dynamic performance deteriorates. Compared with bus A and bus B the acceleration of testbed bus is the worst partly because the response time of the motor is slow because of the heavy weight of the battery pack. Improvement in the performance of fuel cell powered the practical bus A was due to a larger fuel cell, which was the main power source and a battery pack which was the auxiliary power source. The battery pack provided power for the bus when either the fuel cell was starting or when the bus was climbing or accelerating. The battery recovered energy through regenerative braking. This drivetrain belongs to the energy hybrid type also. A Ni/MH battery pack with the capacity of 80 Ah was used, which has a high specific energy and specific power. The practical bus B was equipped with a fuel cell so that its peak power reached 100 kw, and the capacity of the battery was

* Corresponding author. Tel.: +86 29 82668615; fax: +86 29 82665331.
E-mail address: wangjunping@tsinghua.org.cn (J.P. Wang).

0378-7753/$ – see front matter © 2006 Elsevier B.V. All rights reserved.
doi:10.1016/j.jpowsour.2005.12.031

Fig. 1. The developed prototype of fuel cell city bus (from left to right that is testbed bus, practical bus A and practical bus B, respectively).

Table 1
Design parameters of the three fuel cell city bus

Parameter	Value		
	Testbed bus	Practical bus A	Practical bus B
Length × width × height (mm)	11070 × 2490 × 3420		
Tire type	10.00-20-16PR		
Gross weight (no load) (Kg)	12349	12791	12592
Passengers		50	
Gear box ratio	$i_{g1} = 3.002$ $i_{g1} = 3.562$	$i_{g2} = 1.862$ $i_{g2} = 2.036$	2.56
Main reducer ratio	$i_0 = 6.83$		
Fuel cell power (kw)	50	60	100
Battery type	Lithium battery 100Ah	Ni/MH battery 80Ah	Lithium battery 35Ah
Voltage of the battery pack (V)	212	384	336
Motor power (nominal/maximum) (kw)	100/160	60/120	100/120
Motor velocity (nominal/maximum) (r min^{-1})	1780/6000	2000/6000	1800/7200

decreased. The lithium battery pack in this bus had a capacity of only 35 Ah. This drivetrain belongs to the power hybrid type.

Fuel cell powered city bus consists of lots of parts in a complex configuration and has a high safety requirement resulting in difficulty in matching performance requirements. During the development process the experiment on the bus with three types of drivetrain configuration were implemented to optimize the structure and improve performance. To make comparisons with different configurations, three kinds of parameters were introduced: hydrogen consumption, power variation rate of the fuel cell and battery pack and the state of charge (SOC) of the battery pack. The power variation rate is defined as a ratio of the variation of the power to the sampling time. It is simple to measure. The hydrogen consumption and SOC are difficult to measure so we discuss these next.

2. Measurement method of the hydrogen consumption

When hydrogen with mass M is treated as real gas, it follows the Van der Waals equation [2]

$$\left[P + \frac{M^2}{\mu^2}\frac{a}{V^2}\right]\left(V - \frac{M}{\mu}b\right) = \frac{M}{\mu}RT \tag{1}$$

where P is the gas pressure, V the gas volume, T the gas temperature, R the state constant of ideal gas, while the units of

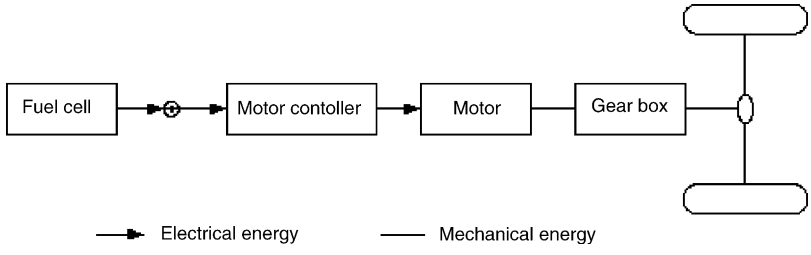

Fig. 2. System configuration with the first-type drivetrain configuration.

gas pressure, volume and temperature are atm, L and K, respectively; R equals 0.0821, a and b are constants, for hydrogen $a = 0.2444\ \text{atm L}^2\ \text{mol}^{-2}$ and $b = 2.65 \times 10{-}5\ \text{L mol}^{-1}$, μ is the mole mass of hydrogen, $\mu = 2$ mol.

For our case $P = 20\ \text{MPa} = 197.43\ \text{atm}$, $V = 900\ \text{L}$, $T = 25\ ^\circ\text{C} = 298.13\ \text{K}$. So the nominal mass of hydrogen in the tank $M = 12.663$ kg. During the experiment we can measure the gas pressure and temperature to estimate the hydrogen consumption by hydrogen mass using Eq. (1). Calculating the mass of the fuel consumed by the integration of fuel temperature and pressure can be unreliable due to the inaccuracies of the sensors involved. To improve the accuracy, the integrated fuel consumption is checked by calculating the total consumption from the initial and final values of the temperature and pressure taken at steady state.

3. Estimation method of state of charge

The SOC of the battery is one of the most important parameters during battery operation and describes the surplus capacity of the battery. The SOC for electric vehicles (EVs) is similar to a fuel gauge in the combustion engine powered car. The voltage, as the criterion, is used to avoid overcharge and overdischarge in early EV usage strategy, but this method did not satisfy the requirement in the bus development, since the battery's current changes drastically in such hybrid electric vehicles (HEV). The accurate estimation of SOC of the battery pack is a key factor in managing batteries with high efficiency. In addition, an accurate estimation of the SOC is also the basis of the power distribution strategy for an HEV. The main SOC estimation approaches include discharge test approach, Ah counting approach, open-circuit voltage approach, load voltage approach, inherent resistance approach, neural networks approach and a Kalman filter approach have all been studied in the literature Lin and Wang [3] and Gregory [5–7]. The Kalman filter approach provides not only the estimated SOC but also the estimation error. This approach is especially suitable for the case of an HEV.

The SOC is a relative quantity that describes a ratio of the remaining capacity to the nominal capacity of the battery. It can be written as

$$S(t) = S(0) - \int_0^t \frac{\eta(t) i(t)}{C} \mathrm{d}t \tag{2}$$

Where $S(t)$ is the SOC at time t, C the nominal capacity, $i(t)$ the current of battery at time t, and η the coulombic efficiency.

3.1. Principle of Kalman filter method

The battery model for a Kalman filter can be written as

$$\left.\begin{aligned} x_k &= f(x_{k-1}, u_{k-1}) + w_k \\ y_k &= g(x_k, u_k) + v_k \end{aligned}\right\} \tag{3}$$

where x_k is the system state vector at time k, u_k the system input at time k, the system output y_k is the battery working voltage, f and g the nonlinear functions specified by the battery model, the system input vector u_k contains the battery current i_k, the battery temperature T_k and the battery capacity C etc. w_k and v_k are the system and measurement noise, respectively.

We constrain the SOC, denoted as S_k, to be a member of the system states x_k, then S_k can be estimated using the extended Kalman filter (EKF) method. For HEV, the current is a dynamic process, and its fluctuating range is very large. Kalman filter is suitable not only for the batteries in an HEV but also for those batteries where the current fluctuation is relatively stable.

3.2. SOC estimation algorithm

The references [5–7] studied the SOC estimation of a LiPB cell based on a Kalman filter, but the research into the battery

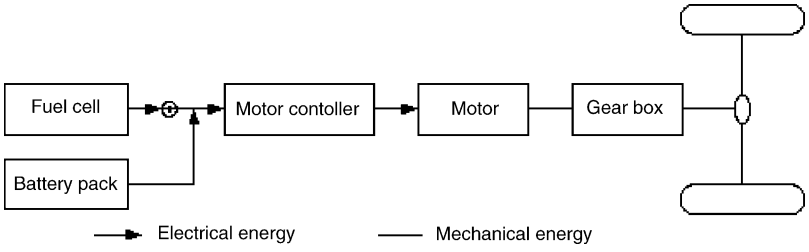

Fig. 3. System configuration with the second-type drivetrain configuration.

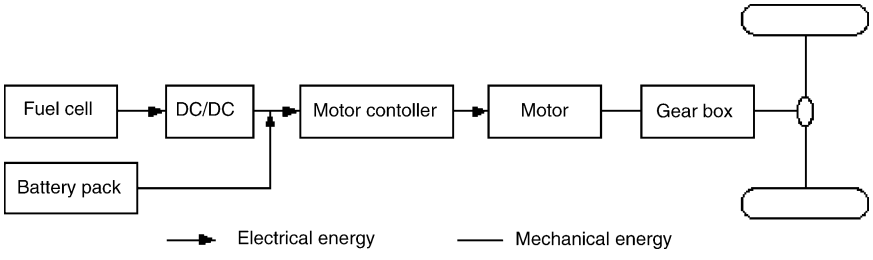

Fig. 4. System configuration with the third-type drivetrain configuration.

Table 2
Experiment results with three types of drivetrain configuration

Parameter	Value				
	Testbed Bus		Bus A	Bus B	
Configuration type	2#	3#	3#	1#	2#
Running time (s)	1200	1780	7394	1500	2975
Average velocity (km h^{-1})	26.1	23.3	26.5	39.5	22.2
Running distance (km)	8.71	11.52	54.38	16.45	18.35
Hydrogen consumption (kg)	0.74	0.8871	4.686	0.8902	0.7919
Top speed (km h^{-1})		62.9	67.6		66
Acceleration time with II gear (0–50 km h^{-1}) (s)		51.2	35.3		30

1# denotes the first-type drivetrain configuration, 2# the second-type drivetrain configuration and 3# the third-type drivetrain configuration.

pack was suitable for the requirement of the vehicle [4,8,11]. The Federal Urban Driving Schedules (FUDS) was used to charge and discharge the battery pack and the battery's state space model with a single state was built, then EKF method can be used to estimate the SOC.

The discrete function of Eq. (3) can be written as

$$S_k = S_{k-1} - \frac{\eta(t) i_{k-1} \Delta t}{C} \tag{4}$$

The measurement equation can be written as

$$y_k = \frac{K_0 - RI_k - K_1}{S_k - K_2 S_k + K_3 \ln(S_k) + K_4 \ln(1 - S_k) + v_k} \tag{5}$$

where R is the internal resistance; K_0, K_1, K_2, K_3, K_4 are the fitting coefficients and the variance of v_k is Q.

The measurement matrix can be deduced from Eq. (5)

$$C_k = \frac{\partial g(I_k, S_k)}{\partial S_k} = \frac{K_1/(S_k)^2 - K_2 + K_3}{S_k - K_4/(1 - S_k)} \tag{6}$$

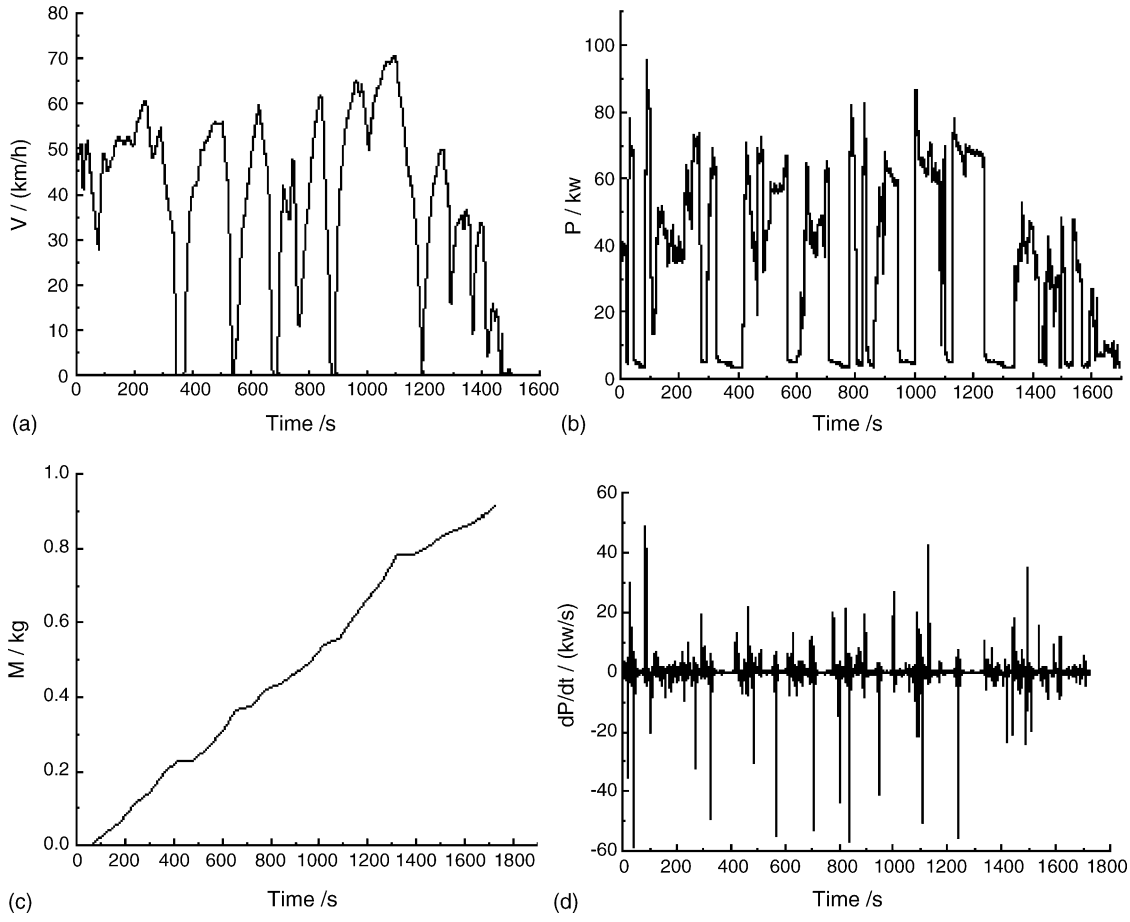

Fig. 5. Test results of the bus B with the first-type drivetrain configuration: (a) velocity profile; (b) power profile of the fuel cell; (c) hydrogen consumption; and (d) the power variation rate of the fuel cell.

The EKF-based SOC estimation algorithm is described as follows

(1) Initialization: given initial value S_0, error covariance matrix p_0 and measurement noise variance Q.
(2) For sampling time $k = 1, 2, 3 \ldots$, sampling battery load voltage y_k, current I_k, the calculation process is iterated as follows.
   - State estimate time update

$$S_{k/k-1} = \frac{S_{k-1/k-1} + \eta i_{k-1}\Delta t}{C} \tag{7}$$

   - Calculating measurement matrix

$$C_k = \frac{K_1/(S_{k/k-1})^2 - K_2 + K_3}{S_{k/k-1} - K_4/(1 - S_{k/k-1})} \tag{8}$$

   - Error covariance time update

$$P_{k/k-1} = P_{k-1/k-1} \tag{9}$$

   - Calculating filter gain matrix

$$L_k = P_{k/k-1}C_k^T[C_k P_{k/k-1}C_k^T + Q]^{-1} \tag{10}$$

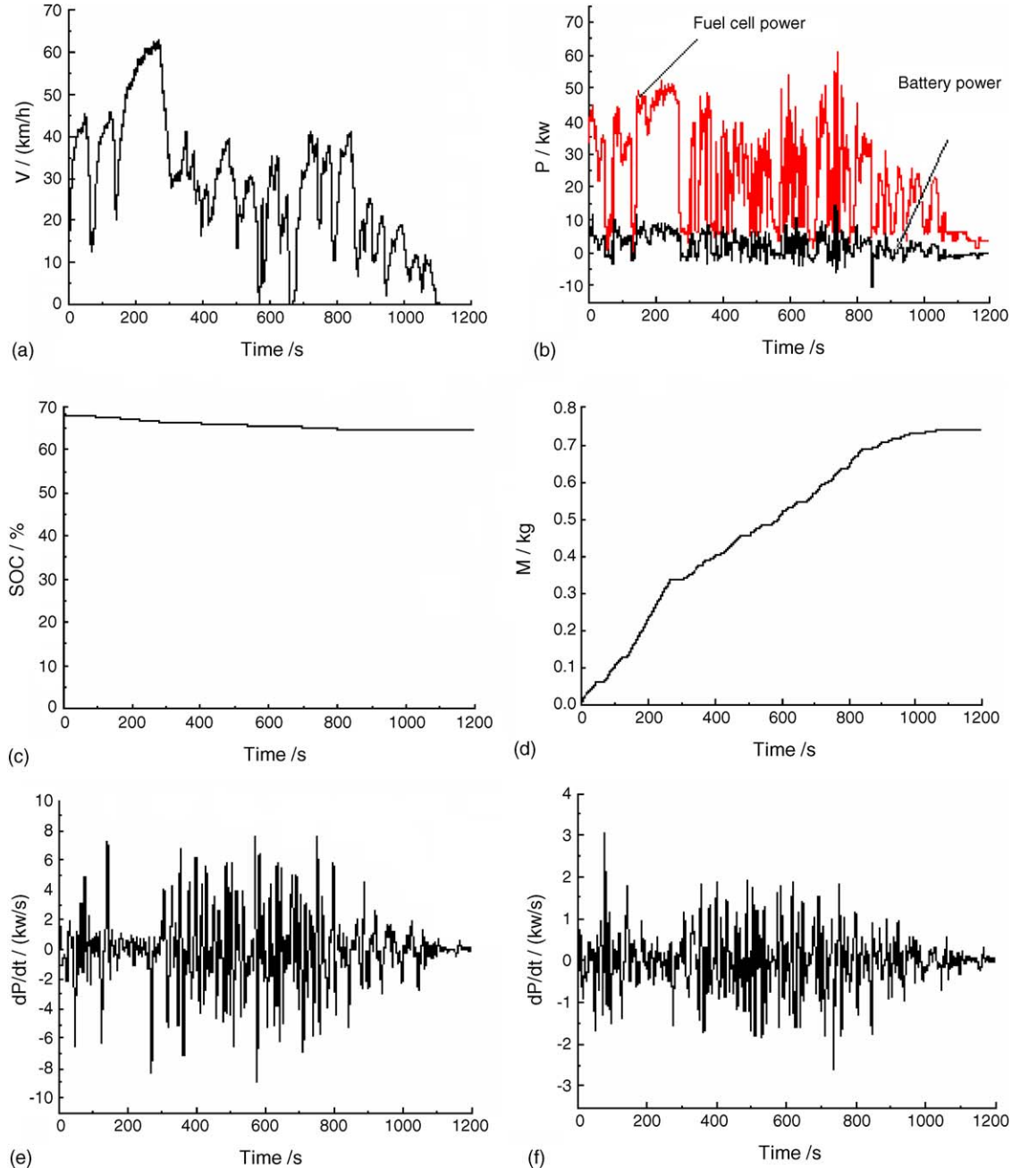

Fig. 6. Test results of the testbed bus with the second-type drivetrain configuration: (a) velocity profile; (b) power profile of the fuel cell and battery pack; (c) SOC of the battery pack; (d) mass of hydrogen consumption; (e) the power variation rate of the fuel cell; and (f) the power variation rate of the battery pack.

- State estimate measurement update

$$S_{k/k} = S_{k/k-1} + L_k[y_k - g(I_k, S_{k/k-1})] \quad (11)$$

- Error covariance measurement update

$$P_{k/k} = (I - L_k C_k)P_{k/k-1} \quad (12)$$

4. Experiment on the fuel cell city bus with different drivetrain configurations

Experiments on the fuel cell city bus with three types of drivetrain configuration were implemented to optimize the structure and improve the performance. The first-type drivetrain configuration is shown as Fig. 2 that the bus was driven by the fuel cell only. The second-type drivetrain configuration is shown as Fig. 3 that the fuel cell links to a battery pack in parallel directly. The third-type drivetrain configuration is shown as Fig. 4 that the fuel cell and DC/DC converter were connected in series with links to the battery pack in parallel. Table 2 shows the comparison of the experimental results and the bus B had the best performance among the three buses. The fuel economy of bus B with the second-type drivetrain configuration was tested during the "2004 Bibendum Challenge" in Shanghai. The bus had run about 111 km with the average velocity of 51.34 km h^{-1}. The fuel economy value was 5.18 kg (100 km)$^{-1}$ and the equivalent gasoline consumption was 19.68 L (100 km)$^{-1}$. So a hybrid fuel

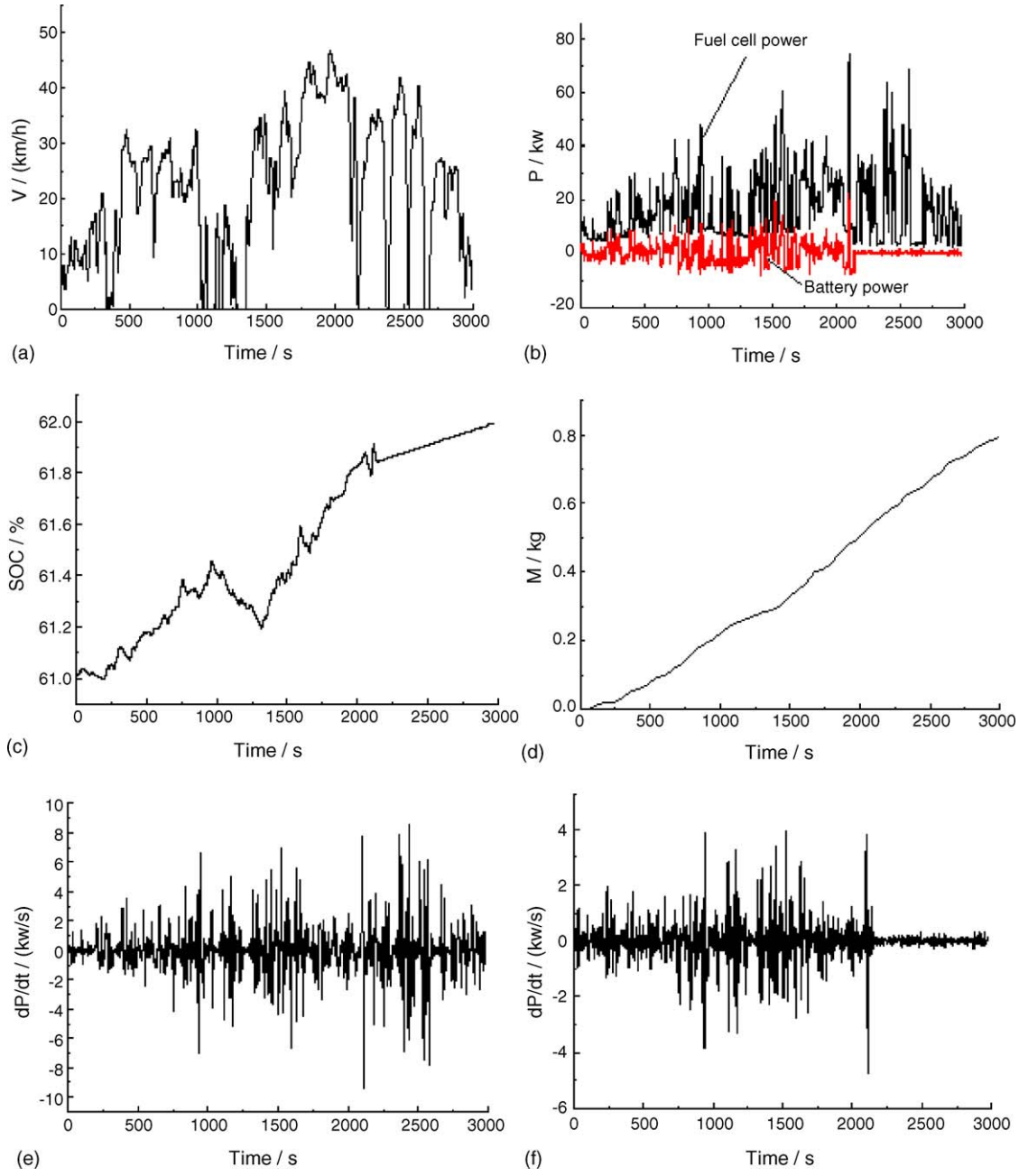

Fig. 7. Test results of the bus B with the second-type drivetrain configuration: (a) velocity profile; (b) power profile of the fuel cell and battery pack; (c) SOC of the battery pack; (d) mass of hydrogen consumption; (e) the power variation rate of the fuel cell; and (f) the power variation rate of the battery pack.

cell city bus has a considerable advantage over the standard ICE version of a city bus in fuel economy.

4.1. Experiment on the bus with the first-type drivetrain configuration

This experiment was carried on the practical bus B and the test results are shown as Fig. 5. The test results show that the power variation rate is drastic and frequent, so it is not good for the fuel cell.

4.2. Experiment on the bus with the second-type drivetrain configuration

In this configuration the power requirement is fulfilled by a fuel cell and battery pack together. First we analyze this configuration theoretically [9].

The relation between the terminal voltage of the fuel cell V_{FC} and current I_{FC} is

$$V_{FC} = V_{FC0} - b\log\left(\frac{I_{FC}}{A_{FC}}\right) - R_{FC}I_{FC} \quad (13)$$

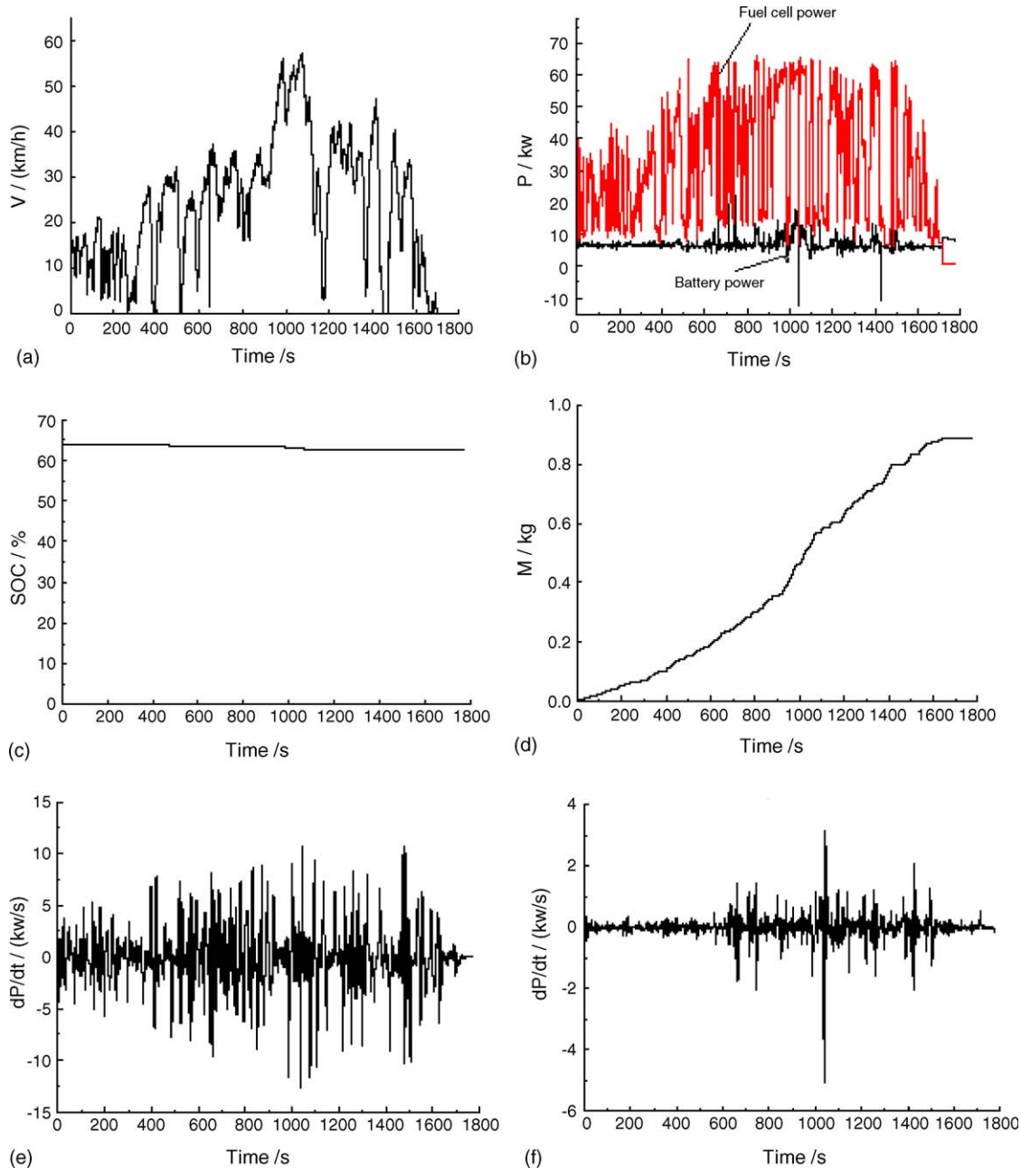

Fig. 8. Test results of the testbed bus with the third-type drivetrain configuration: (a) velocity profile; (b) power profile of the fuel cell and battery pack; (c) SOC of the battery pack; (d) mass of hydrogen consumption; (e) the power variation rate of the fuel cell; and (f) the power variation rate of the battery pack.

Where V_{FC0} is the open-circuit voltage, b the Tafel slope, A_{FC} the cross area of the fuel cell and R_{FC} the internal resistance of fuel cell.

If a simple model of battery pack is used, the relation between terminal voltage V_B and current I_B of battery pack is

$$V_B = V_{B0} - R_B I_B \tag{14}$$

where R_B is the internal resistance of the battery and V_{B0} the open-circuit voltage.

The fuel cell links the battery in parallel directly, so $V_{FC} = V_B$, we can get

$$I_B = \frac{b\log(I_{FC}/A_{FC}) + R_{FC}I_{FC} - (V_{FC0} - V_{B0})}{R_B} \tag{15}$$

From Eq. (15) we know that the larger the difference between V_{B0} and V_{FC0}, the larger the output current of the battery. While R_B is small, the output current of the battery is large. The energy distribution is determined by the parameters of the fuel cell and the battery pack at the design stage, so the distribution is fixed, which cannot be adjusted online.

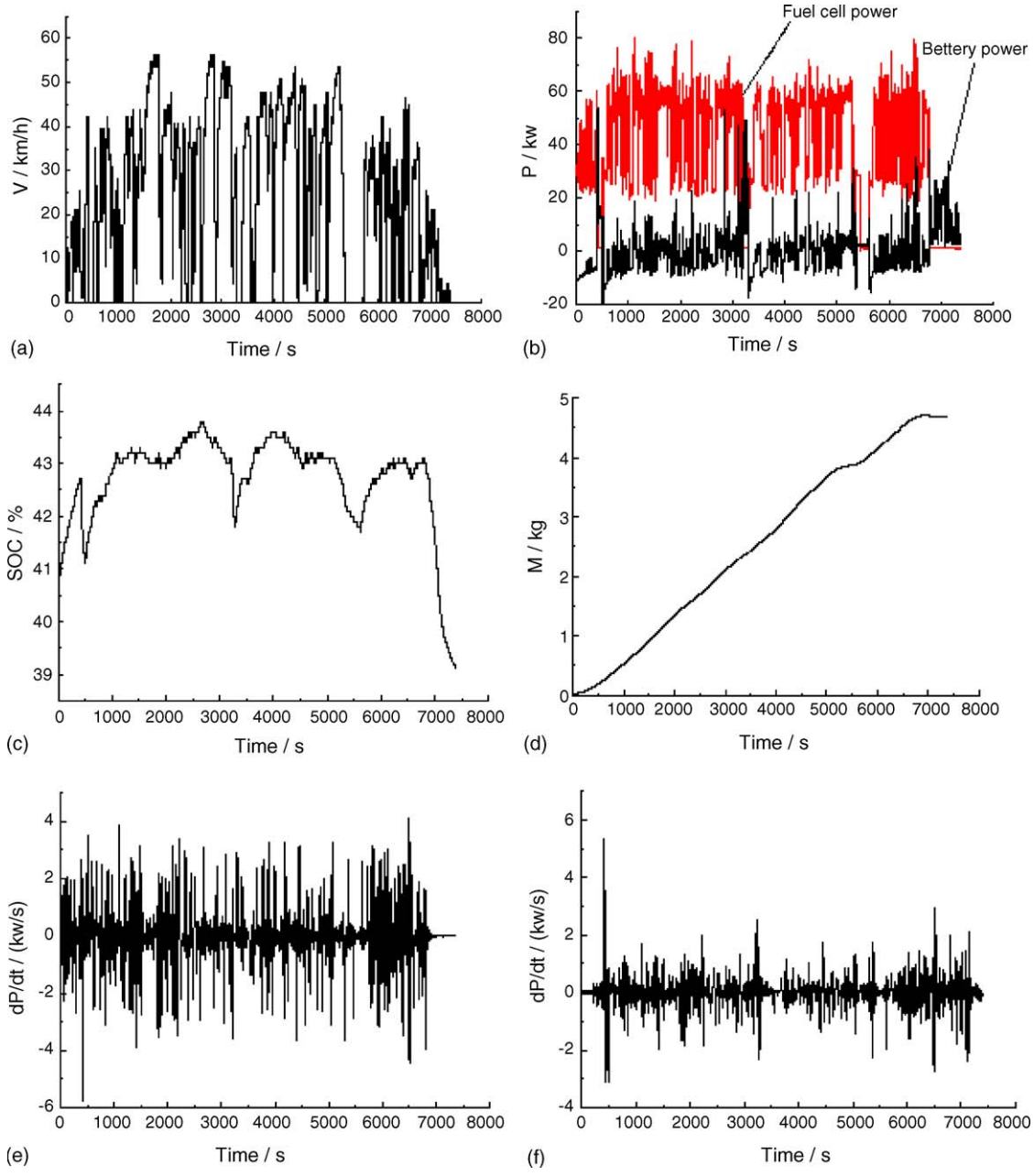

Fig. 9. Test results of the bus A with the third-type drivetrain configuration: (a) velocity profile; (b) power profile of the fuel cell and battery pack; (c) SOC of the battery pack; (d) mass of hydrogen consumption; (e) the power variation rate of the fuel cell; and (f) the power variation rate of the battery pack.

This experiment was carried on the testbed bus and the practical bus B, respectively. The test results are shown as Figs. 6 and 7. Fig. 6 shows the test results for the testbed bus with the second-type drivetrain configuration. Fig. 7 shows the test results of the bus B with the same configuration. The power variation rate was reduced apparently compared with the case driven only by fuel cell, but the power variation magnitude of the fuel cell was larger than that of battery pack.

Compared with the testbed bus, the practical bus B was driven by a larger power fuel cell and the capacity of the battery pack was decreased. Under the condition of an approximately similar amount of hydrogen consumption, bus B has almost two times the running distance than that of the testbed bus. This is attributed to the significant improvement of the fuel cell and motor control technology and to the larger fuel cell with a lower average current density, and hence a more efficient voltage operation. The battery pack was charged by the fuel cell frequently so the SOC of the battery increased.

4.3. Experiment on the bus with the third-type drivetrain configuration

In this configuration, the power requirement was fulfilled by a fuel cell and battery pack together. The output voltage of the fuel cell is the input voltage of the DC/DC converter [10]. For the DC/DC converter in parallel with the battery pack, the output voltage of the DC/DC converter was $V_{DC} = V_B$. The entire current of the parallel circuit I is

$$I = I_{DC} + \frac{V_{B0} - V_{DC}}{R_B} \tag{16}$$

where I_{DC} is the output current of the DC/DC converter. Setting the output current or voltage of the DC/DC converter, output current of the battery pack and the energy distribution are carried out online.

This experiment was carried out on the testbed bus and the practical bus A, respectively. The test results are shown as Figs. 8 and 9. Fig. 8 shows the test results of the testbed bus with the third-type drivetrain configuration. Fig. 9 shows the test results of the bus A with the same configuration.

The power variation rate of the fuel cell was reduced apparently because of the DC/DC converter. The power variation rate of the battery pack was also reduced. The SOC of the battery can be adjusted according to requirements by controlling the DC/DC converter. The hydrogen consumption was larger in bus A.

5. Conclusions

Three fuel cell city buses were developed, which belong to energy hybrid- and the power hybrid-type, respectively. Experiments on the fuel city bus with three types of drivetrain configurations were implemented to optimize the structure and improve the performance. Energy distribution, hydrogen consumption, SOC and the power variation rate were analyzed when different drivetrain configurations and parameters were used.

When driven only by a fuel cell, the bus cannot recover the energy through regenerative braking. The variation of the fuel cell power in this case is drastic and frequent, so it is not good to the fuel cell. When a fuel cell is linked to a battery pack in parallel, the bus can recover the energy through regenerative braking. The energy distribution is determined by the parameters of the fuel cell and the battery pack at the design stage. The power variation rate of the fuel cell was thereby reduced. When the fuel cell and DC/DC converter are connected in series, and the battery pack is in parallel, energy can be recovered and the energy distribution can be adjusted online. The power variation rate of both the fuel cell and the battery pack were reduced apparently.

Acknowledgements

The research was supported by a grant from the National High Technology Research and Development Program of China (No. 2003AA501100) and the research fund of State Key Laboratory of Automobile Safety and Energy Conservation (No. KF2005-006 & KF2005-007). The authors would like to express their thanks for the fund. This experiment was done when the first and second author being post doctoral position in Tsinghua University and the authors would like to express their thanks to all team members.

References

[1] Jayson Cannon, Paul B. Scott, Hybrid-electric fuel cell bus demonstration, in: Proceedings of the 20th International Electric Vehicle Symposium, California, EVAA, 2003, (CD-ROM).
[2] C. Li, L. Zhang, S. Qian, Calorifics, People's Education Press, Beijing, 1978.
[3] C.T. Lin, J.P. Wang, Methods for state of charge estimation of EV batteries and their application, Battery 34 (2004) 376–378.
[4] J.P. Wang, Q.S. Chen, B.G. Cao, et al., Study on the charging and discharging model of Ni/MH battery module for electric vehicle, J. Xi'an Jiaotong Univ. 40 (1) (2005) 50–52.
[5] L.P. Gregory, Extended Kalman filtering for battery management systems of LiPB-based HEV battery packs Part 1:background, J. Power Sources 134 (2) (2004) 252–261.
[6] L.P. Gregory, Extended Kalman filtering for battery management systems of LiPB-based HEV battery packs Part 2: modeling and identification, J. Power Sources 134 (2) (2004) 262–276.
[7] L.P. Gregor, Extended Kalman filtering for battery management systems of LiPB-based HEV battery packs Part 3: state and parameter estimation, J. Power Sources 134 (2) (2004) 277–292.
[8] J.P. Wang, Q.S. Chen, C.T. Lin, Study on estimating of the state of charge of Ni/MH battery pack for electric vehicle, Chin. J. Mech. Eng. 41 (12) (2005) 62–65.
[9] Chen Yong, Vehicle design and experimental study on fuel cell city buses, Post doctor Research Report, Tsinghua University, 2004.
[10] Denis Candusso, Ianko Valero, Aurelien Walter, Modelling, control and simulation of a fuel cell based power supply system with energy management, in: Proceedings of the IEEE the 28th Annual Conference of the Industrial Electronics Society, 2002, pp. 1294–1299.
[11] J.P. Wang, Q.S. Chen, B.G. Cao, Support vector machine based battery model for electric vehicles, Energy Conversion Manage. 47 (7) (2006) 858–864.